

LIDAR-Assisted Channel Modelling for LiFi

Sreelal Maravanchery Mana, Kerolos Gabra Kamel Gabra, Sepideh Mohammadi Kouhini, Malte Hinrichs, Dominic Schulz, Ronald Freund, Volker Jungnickel

Fraunhofer Heinrich-Hertz Institute (HHI), Einsteinufer 37, 10587 Berlin, Germany
sreelal.maravanchery@hhi.fraunhofer.de

Abstract: We present fast and accurate modelling of LiFi channels using data from LIDAR scans. Line-of-sight, first and residual reflections are modelled in the frequency-domain and using the integrating-sphere method. Model and measurement show good agreement. © 2022 The Author(s)

1. Introduction

Mobile optical wireless communications, which is also denoted as LiFi, gains interest in many applications [1]. LiFi systems work efficiently through the line-of-sight (LOS) and first non-LOS (NLOS) reflections. Deployment of LiFi in complex scenarios is challenging due to potential link blockages, besides reflections from objects and walls. Distributed multiple-input multiple-output (MIMO) approaches were shown to be effective against blockages [2]. However, for the large number of MIMO links, efficient channel modelling is needed which includes these effects.

The LiFi channel depends on the geometrical properties of the room and the parameters of optical frontends. In the literature, at first, each object in the room is modelled manually [3-6]. This is time consuming and lacks the precision needed to determine the availability of the LOS. Secondly, ray tracing is used to obtain the channel impulse response [3]. Due to complexity, both steps are hardly practical to model the LiFi channel along arbitrary traces for multiple mobile users in distributed MIMO scenarios. These scenarios call for reduced complexity.

LIDAR is widely used to scan the 3D scenario in which mobile communication systems are deployed [7]. Here, we adopt this approach and use 3D geometrical data from LIDAR as an input for LiFi channel modelling, for the first time. Secondly, we use a recently introduced frequency-domain (FD) method to model the LOS and the initial NLOS reflections precisely [4]. FD simulation is inherently faster, but similarly accurate like ray tracing. Third, we use the well-known integrating sphere model [5] for the residual higher order reflections, as outlined in [8]. In this paper, we combine all these ideas for the first time and demonstrate that our advanced method is similarly precise but computationally more efficient to model the LiFi channel in real scenarios. We show that the simulated channels and throughputs in a mobile MIMO LiFi scenario agree very well with measurements.

2. 3D modelling using LIDAR

To capture the indoor environment, a LIDAR scanner is placed and scanned in multiple locations. Each output data file from the LIDAR consists of the 3D coordinates of the detected points and the intensity value of the beam reflected at these points. Before using this data as an input to the channel modelling algorithm, post processing of the point cloud data has been done to remove noisy points, reduce the point resolution and calculate the surface

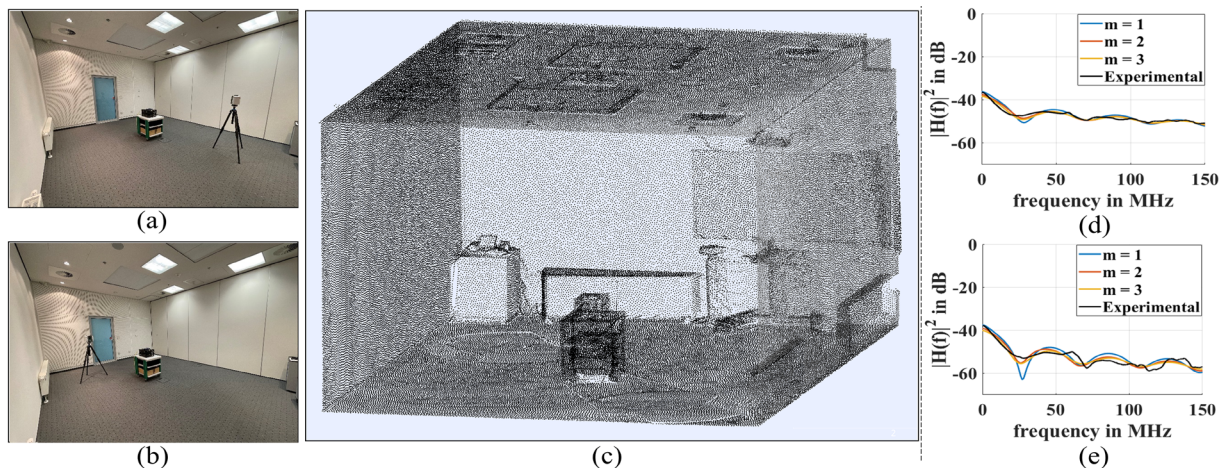


Fig. 1. (a) LIDAR scanner (Leica RTC360) at position 1 and (b) at position 2. (c) Point cloud data of the room after LIDAR data processing as seen from the door side. (d) Magnitude response of NLOS LiFi channels versus frequency at 2.5 m distance and (e) at 3 m distance, respectively, where m is the order of reflections modelled precisely by the frequency-domain method.

normal. Furthermore, the reflectance parameters of the surface points are calculated from the intensity data using a general LIDAR equation [9]. Afterwards, all the scanned data are merged to get the complete point cloud data of the room. Finally, the processed LIDAR data set is then provided as the input into the channel modelling algorithm.

3. Channel Modelling Methodology

The elementary LOS channel response between transmitter (Tx) and receiver (Rx) is given as

$$H(f) = V_{Tx,Rx} \cdot L_{Tx,Rx} \cdot e^{-j2\pi f T_{Tx,Rx}} \quad (1)$$

where $T_{Tx,Rx}$ is the delay time and $L_{Tx,Rx}$ is the transfer coefficient between Tx and Rx [4]. The visibility factor $V_{Tx,Rx}$ is equal to one if there is a free LOS between Tx and Rx and it is equal to zero otherwise. Next, we model the first NLOS reflections using the FD method [4]. We consider the reflecting surfaces as N surface elements, each represented by its center position. This approach assembles all mutual LOS links between all surface elements as well as the links between the surface elements to the Rx and Tx in a matrix form and to compute NLOS reflections by consecutive matrix multiplications [8]. Each element in these matrices contains an additional factor, which defines the visibility in the link similar to equation (1). Visibility analysis of point cloud data is a well-known problem in the fields of computer graphics and photogrammetry. Among many methods, use of the hidden point removal operator yields a simple and fast method to determine the visible points in a point cloud data set from a given viewpoint [10]. By replacing the view point by Tx, Rx or surface point locations, we can estimate how many points are visible from each location. Using the same method, we can also estimate the visibility in the link between each Tx and each Rx. Finally, the residual diffuse reflections are calculated using Ulbricht's integrating sphere model [5]. This model includes basic parameters of the room (volume, surface etc), which can be easily obtained from the LIDAR data. Finally, the complete LiFi channel model is obtained, by adding the LOS and all NLOS signals [8].

4. Measurements

To test the accuracy of our new method, we have conducted measurements in an empty room scenario with the size of 5.8 m x 4.5 m x 3.1 m. At first, the LIDAR scanner (Leica RTC360) is placed at two positions as shown in Fig. 1(a) and Fig. 1(b) and each scan data set is processed. The two processed point cloud data are merged as shown in Fig. 1(c). This data set is used as an input to our channel model algorithm, along with optical frontend parameters. In order to validate simulation results, we perform channel measurements in the same room with our MIMO LiFi channel sounder [2, 11]. It uses a multi-carrier approach for simultaneous measurement of MIMO LiFi channels [2]. Calibration and post-processing of the channel measurement data are done to get the final channel responses, as described in [11].

5. Results

In this section, we report the measurement and simulation channel responses for different Tx and Rx configurations. At first, to check the accuracy of NLOS channels, we consider previously reported two NLOS scenarios with dominant first-order reflection [12]. The simulated and experimental magnitude responses of the LiFi channels are shown in Fig. 1(d) and Fig. 1(e). In this NLOS scenario, Tx and Rx are looking towards the ceiling and the distance of separation is 2.5 m (in Fig. 1(d)) and 3 m (in Fig. 1(e)). To compare the accuracy of the method, concerning the number of first reflections, we increased the reflection order m in FD method [4] from 1 to 3 and calculated channel responses. We observe that for the 3 m scenario the mean square error (MSE) is 10%, 4% and 3% for the reflection order $m = 1, 2,$ and 3 cases when compared to the experimental result. Similarly, for 2.5 m scenario, the MSE is 2.6%, 1.1% and 0.8% for $m = 1, 2$ and 3. Therefore, as the reflection order m increases, the simulation results are in better agreement with the experimental results. In the rest of our simulations, we model the first three reflections using the FD method and the remaining reflections using the integrated sphere method.

Now, in the same room, we perform the 4x4 MIMO channel measurement. As shown in Fig. 2(a), all transmitters are kept at a 2 m x 2 m grid configuration and each Rx is kept at the middle position of two transmitters. The measurement and simulation results are shown in Fig. 2(b)-(e). Here, the bold line denotes the measured responses and the dotted line denotes the simulated responses. Due to small mismatching in the optical frontends, wires and connectors, the measured responses always have minor differences from each other and do not overlap like the simulated curves. In addition, the measurement results are significantly affected by the noise when the channel response is below -35dB. From the results, we observe that MSE is less than 3% for channels with good signal strength and 10% to 30% for weak signals.

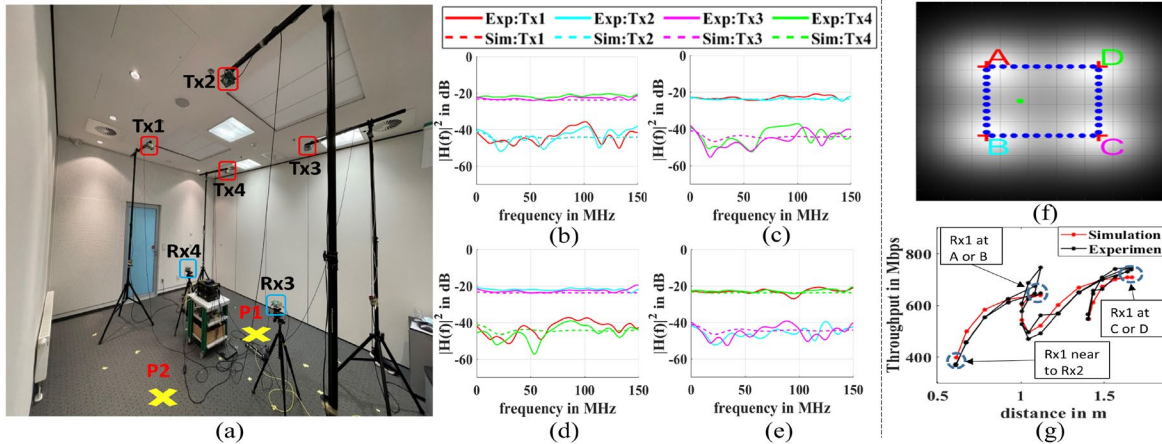


Fig. 2. (a) 4x4 MIMO configuration in the room. P1 and P2 represent the position of Rx1 and Rx2, which have been measured separately. Subfigures (b), (c), (d) and (e) represent the magnitude responses of LiFi channels at Rx1, Rx2, Rx3 and Rx4 versus frequency for all transmitters. (f) Top view of optical power distribution in the room. A,B,C and D represent locations of Tx1, Tx2, Tx3 and Tx4. Blue and green colors indicate Rx1 (mobile) and Rx2 locations. (g) Simulated and measured throughputs versus distance between Rx1 and Rx2. Dash line circles indicate throughput with respect to the position of Rx1 (mobile).

Finally, we consider a mobile MIMO scenario like in [8]. As shown in Fig. 2(f), Rx1 is moving on a track to 40 different positions (marked as blue color dots) while the Rx2 is kept stationary (marked as green color dot). We have compared the channel gain along the track and observed similar good agreement between simulations and measurement. Moreover, we study the achievable data rate in a distributed multiuser MIMO link with 4 Txs and 2 users. Based on the modified Foschini formula (see equation (2) in [12]), the sum throughput for both Rxs is calculated along the track as shown in Fig. 2(g). While Rx2 is fixed, Rx1 moves as follows: first from A to B, then B to C, next C to D and finally D to A. Both the received power and the structure of the MIMO channel matrix have an impact on the results. Data rate is lowest when both receivers are close to each other and Rx1 has minimum power. Minima occur always if the Rx1 is between two points A, B, C or D. Data rate is the highest if Rx1 is in points C and D. The intermediate maxima occur when Rx1 is next to points A or B where power is similar like in points B and D but the two Rxs are nearer to each other, which leads to a reduced channel rank. Overall throughput results show good agreement. In the measurement, we observe occasional overestimation of the throughput, due to the noise. However, the comparison of simulated and measured throughput results yields the MSE below 5%.

6. Conclusions

We have shown how to model the LiFi channel with high accuracy and low complexity for mobile users in a real distributed MIMO scenario. First, we obtained the 3D environment from a LIDAR scan and then use these data directly to generate the MIMO channel matrix, including the LOS and all NLOS reflections. We found good agreement with MSE of less than 5 percent between the model and measurements, both on single links and in analyzing the performance of a distributed multiuser MIMO link. Our new approach allows accurate and efficient performance prediction of LiFi systems in complex scenarios. Another application is LiFi network planning in real deployment scenarios.

7. Acknowledgement

This research is funded by the European Union in the VISION ITN project, under the grant agreement no: 764461.

8. References

- [1] H. Haas et al., "What is LiFi?", *J. Lightwave Technol.*, vol. 34, no. 6, pp. 1533-1544, Mar. 15, 2016.
- [2] P. W. Berenguer et al., "Optical Wireless MIMO Experiments in an Industrial Environment", *IEEE JSAC*, vol.36, pp. 185-193, Jan. 2018.
- [3] F. Miramirkhani et al. "Channel modelling for indoor visible light communications", *Phil. Trans. R. Soc.* 2020.
- [4] H. Schulze, "Frequency-domain simulation of the indoor wireless optical communication channel", *IEEE TComm.*, vol. 64, June 2016.
- [5] V. Jungnickel et al., "A physical model of the wireless infrared communication channel", *IEEE JSAC.*, 2002, 20, (3), pp. 631–640.
- [6] S.P.Rodríguez et al., "Simulation of impulse response for indoor visible light communications using 3D CAD models", *EURASIP JWCN* 2013.
- [7] J. Järveläinen et al., "Indoor Propagation Channel Simulations at 60 GHz Using Point Cloud Data", in *IEEE TAP*, vol. 64, Oct. 2016.
- [8] S. M. Mana et al., "An Efficient Multi-Link Channel Model for LiFi", *IEEE PIMRC* 2021.
- [9] Jelalian, A., 1992. *Laser radar systems*. Artech House, Boston London.
- [10] S. Katz et al., "Direct Visibility of Point Sets," *ACM Trans. Graphics*, vol. 26, no. 3, p. 24, 2007.
- [11] S. M. Mana et al. "Distributed MIMO Experiments for LiFi in a Conference Room," *CSNDSP*, 2020.
- [12] S. M. Mana et al., "Experiments in Non-Line-of-Sight Li-Fi Channels", in 2019 *Global LIFI Congress (GLC)*, Paris, France, pp. 1-6, 2019.